Journal of Ceramic Processing Research. Vol. 5, No. 1, pp. 64~69 (2004)

J O U R N A L O F
Ceramic Processing Research

Residual stresses in ceramic nanocomposites and their determination by Raman spectroscopy

Henryk Tomaszewski* and Jan Strzeszewski[a]
Institute of Electronic Materials Technology, Wolczynska 133, 01-919 Warsaw, Poland
[a]Institute of Physics, Warsaw University of Technology, Koszykowa 5, 00-662 Warsaw, Poland

Residual stresses in ceramics, as for example arising from thermal expansion anisotropy, exert an important influence on the mechanical behaviour of polycrystalline materials. They can lead to crack initiation in the sense of microcracking but can also influence crack propagation by determining the evolution of the crack path and contribute to the effectiveness of crack bridging or by microcrack shielding. Various methods have been utilised to measure residual stresses. In this paper, a method based on the piezospectroscopic (PS) effect is discussed by application to Ce-ZrO_2/Al_2O_3 nanocomposites having 0-90 vol. % of alumina. The compressive stress in Al_2O_3 was determined from the frequency shift of the R_2 luminescence band using the well-known piezospectroscopic coefficient. The tensile stress in t-ZrO_2 has been found in two ways. In the first one, it has been derived from the equilibrium of forces in a free-standing piece of two-phase material. The frequency shifts of each Raman band of t-ZrO_2 have been plotted against the calculated stress and the slopes provided the PS coefficients. In the second method, external compressive stress introduced into composite samples by Vickers indentation was used for a new PS calibration due to a linear dependence observed between the t-ZrO_2 Raman line shift for all Raman lines of zirconia and those of the Al_2O_3 R_2-line luminescence. This way, having new PS coefficients a new value of stress in t-ZrO_2 was calculated. Good correspondence of PS and stress in t-ZrO_2 obtained from these two methods was found. As a result new indirect methods for determining PS coefficients of t-ZrO_2 are suggested.

Key words: ceramic nanocomposites, residual stresses, Raman spectroscopy, piezospectroscopic coefficients.

Introduction

Residual stresses in ceramics, as for example arising from thermal expansion anisotropy, exert an important influence on the mechanical behaviour of polycrystalline materials. They can lead to crack initiation in the sense of microcracking [1] but can also influence crack propagation by determining the evolution of the crack path [2, 3] and contribute to the effectiveness of crack bridging [4, 5], or by microcrack shielding [6].

Various methods have been utilised to measure residual stresses. In this study, the residual stresses in composites of Ce-ZrO_2/Al_2O_3 were determined using the piezospectroscopic (PS) effect. This phenomenon is based on the known relationship between the value of some particular spectroscopic parameter and the stress state to which the material is subjected:

$$\Delta\nu=\Pi_{ij}\sigma_{ij} \quad (1)$$

where $\Delta\nu$ represents the frequency shift calculated with respect to an assumed stress-free reference state, Π_{ij} is the tensor of the derivatives of the frequency shifts with respect to stresses, σ_{ij}, applied along the axis of the crystallographic system; Π_{ij} is called the tensor of the piezospectroscopic coefficients.

Stress information from the experimentally observed frequency shift $\Delta\nu$ is based upon the knowledge of the piezospectroscopic coefficients. Usually these are determined by a calibration procedure whereby the sample is stressed to a known extent and the corresponding spectrum is then recorded [7]. This procedure requires a loading device that must be stiff and able to be fitted under the microscope objective lens. Moreover, since the stress is derived from the applied load through the standard elastic solutions, the samples must have carefully controlled shape and dimensions.

In this paper two different methods for determining PS coefficients and then stresses in two phase/material composite are reported, which require any type of loading device nor any precise machining of the ceramic sample. Both methods are based on the mixture of two phases/materials, when the PS coefficient and stress in one phase/material is independently known.

Experimental procedure

Zirconia/alumina composite samples having 0-90 vol% of alumina were prepared following a standard ceramic preparation procedure. First starting powders: Ce-ZrO_2 containing 12 mol% of CeO_2 (CEZ-12, Mandoval

*Corresponding author:
Tel : +48-22-835-39-41
Fax: +48-22-834-90-03
E-mail: henryk.tomaszewski@iteme.edu.pl

Limited, UK) and alumina (AKP-53, Sumitomo, Japan) were homogenised 24h in distilled water. Then the mixed powder compositions were dried, uniaxially pressed, isopressed and sintered at 1600°C for 2h. For comparison pure zirconia and pure alumina samples were prepared under the same conditions.

The Cr^{+3} luminescence and the Raman measurements were performed using a micro-Raman set-up containing a triple spectrometer (DILOR XY) with a liquid-nitrogen cooled CCD (charge couple device) detector and an optical microscope. A 50x objective with a 0.55 numerical aperture was used to focus the incident light on a spot of about 100 μm in diameter and to collect the light in back scattered geometry. The scattering light was excited by the 488 and 514.5 nm lines of an Ar^{+} laser. To avoid overheating of the samples the output laser power was kept below 40 mW. The Si Raman line at 520 cm^{-1} was used for wavenumber calibration of the Raman spectra, whereas the lines of a neon lamp were used to calibrate the Cr^{+3} luminescence. Peak positions were obtained by fitting the spectra to a special computer program. The frequency shifts mentioned throughout the paper have been obtained by subtracting from the peak frequency of the sample under investigation the peak frequency of the stress-free reference samples.

To calibrate the stress dependence of the Raman shift in the second of the methods offered a Vickers indentation (10 kg load) was prepared in the composites studied. Along this external compressive stress field both spectra: luminescence and Raman were collected at the same place of the sample at a distance of 0-300 μm from the indent. An example of the indent is shown in Fig. 1. Two fringes observed on the optical interference micrograph of the Vickers indent are a result of the optical system in Nomarsky interferometer of our Reichert microscope MeF2.

Results and Discussion

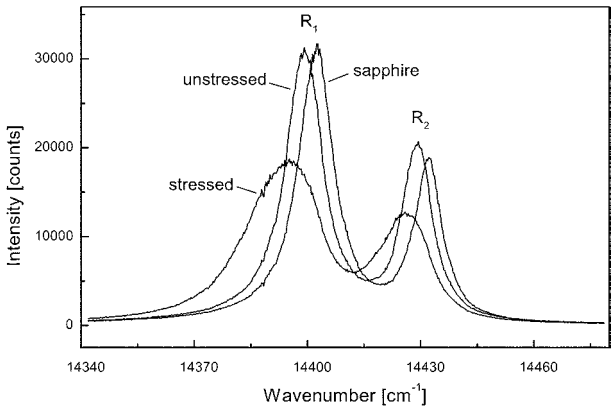

Fig. 2. Luminescence spectra of Ce-ZrO_2/Al_2O_3 (60 vol.%) composite taken close to ("stressed") and far from the indentation ("unstressed"). For comparison spectra of unstressed sapphire is added.

The coefficient of thermal expansion of t-ZrO_2 is greater than that of Al_2O_3 ($\alpha_{Al_2O_3}$=9.0×10^{-6} °K^{-1}, α_{ZrO_2} =12.0×10^{-6} °K^{-1}); thus alumina is expected to be in compression but zirconia in tension independent of Al_2O_3 content in composites studied when cooled from the fabrication temperature. This expectation was confirmed by luminescence and Raman spectras. An example of the luminescence of the R-lines for a Ce-ZrO_2/Al_2O_3 composite containing 60 vol.% of alumina (described as an unstressed spectra) is shown at Fig. 2. For comparison the spectra of sapphire is added. The R-lines of the composite move to a lower wavenumber, which means the presence of compressive stress.

As is generally known there are two factors responsible for residual stresses in alumina grains: a difference in thermal expansion of Al_2O_3 and ZrO_2 and crystallographically anisotropic thermal expansion of the Al_2O_3. However, the contribution of the first reason seems to be dominant in composite samples and strongly increases with zirconia content (Fig. 3). Equation

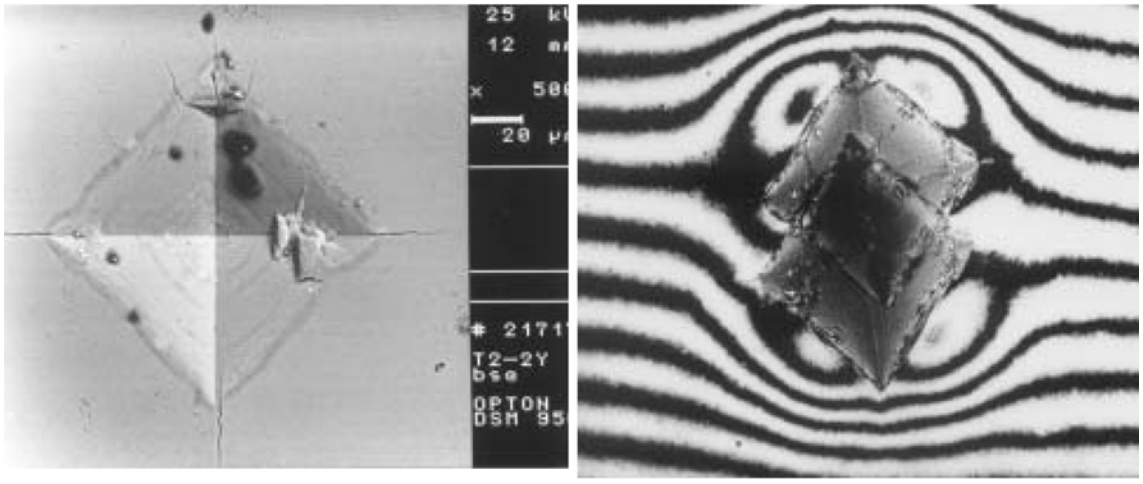

Fig. 1. An example of scanning microscope (left) and optical interference (right) micrographs of Vickers indent made in zirconia ceramics.

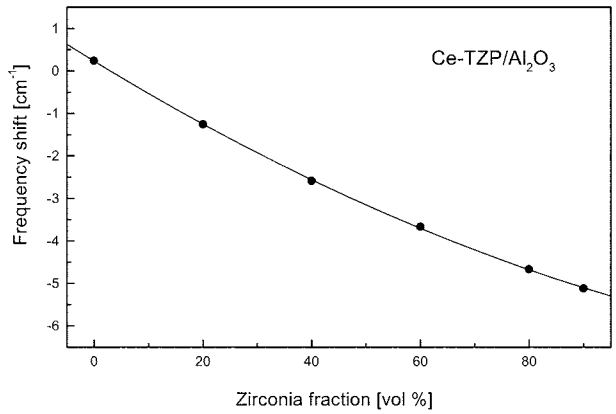

Fig. 3. Frequency shift of the R_2 luminescence line of Al_2O_3 as a function of zirconia content in Ce-ZrO_2/Al_2O_3 composites.

Table 1. Comparison of residual stresses in alumina and zirconia obtained from different piezospectroscopic methods

Hydrostatic stress, MPa	Zirconia content in composite, vol.%					
	0	20	40	60	80	90
Al_2O_3 (from luminescence)	+32	-166	-340	-482	-614	-673
Al_2O_3 (from Raman)		-140	-300	-500		
ZrO_2 (from balance formula)		+664	+510	+321	+153	+75
ZrO_2 (from Raman)		+680	+493	+315	+153	+85

1 was applied to derive the stress in alumina using the experimental frequency shift of the R_2 luminescence band in the various samples and the well known PS coefficient of this band, Π=7.6 cm^{-1}/GPa [8, 9]. The compressive stress in alumina in a function of zirconia content is presented in Table 1. According to the first method proposed the stress in t-ZrO_2 was calculated on the base of the equilibrium forces in free-standing piece of composites given by:

$$f_{ZrO_2}\langle\sigma\rangle_{ZrO_2}+f_{Al_2O_3}\langle\sigma\rangle_{Al_2O_3}=0 \quad (2)$$

where f_{ZrO2} and f_{Al2O3} represent the volume fraction of both phases (see Table 1). The position of all Raman lines of t-ZrO_2 shifts with alumina content to higher frequencies (Fig. 4). The only exception is the line observed at 260 cm^{-1}, which moves toward higher energies. Finally the Raman shift of all t-ZrO_2 bands are graphed as a function of the stress $\langle\sigma\rangle_{ZrO_2}$. These graphs are presented in Fig. 5. The slope of the best fitting lines (Fig. 6) yields the PS coefficients of the corresponding Raman bands reported in Table 2, together with the values for the same bands determined by other researchers. The PS coefficients of t-ZrO_2 stress in zirconia have been calculated using eq. 1 and given in Table 1. As can be seen values of stress are comparable, independent of the calculation method. The same method of calculation was used for alumina. Two alumina peaks observed at 355 and 417 cm^{-1} are visible in the Raman spectrum of composites (Fig. 7). Their intensity is small in comparison with pure alumina

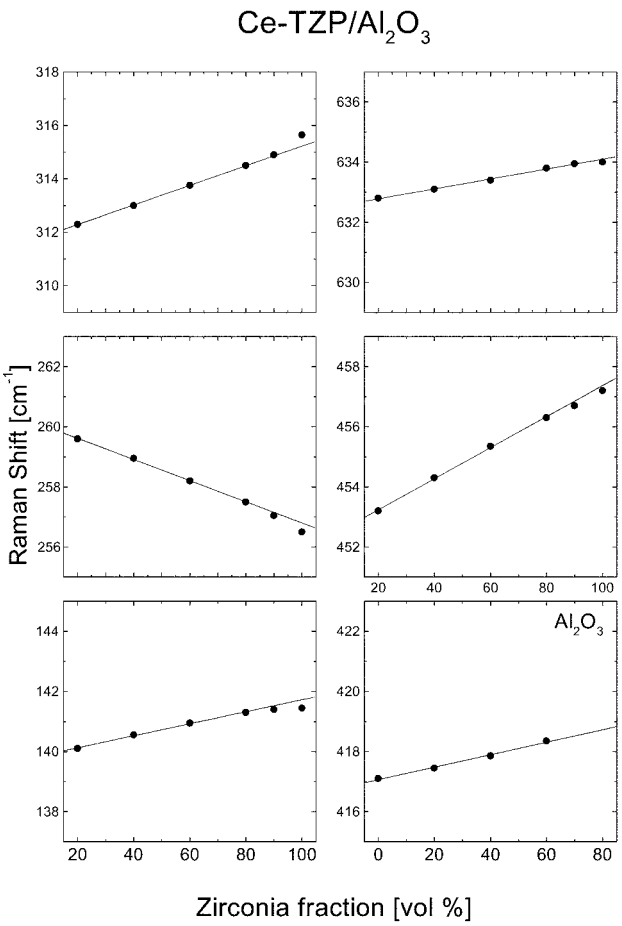

Fig. 4. Raman lines position of t-ZrO_2 for different zirconia content in Ce-ZrO_2/Al_2O_3 composites. In the right bottom part of the picture the same is shown for 417 cm^{-1} line of Al_2O_3.

but rises with alumina content. The most active Raman mode of Al_2O_3 at 417 cm^{-1} shifts with stress (Fig. 5). Its PS coefficient is given in Table 2.

To extend the internal stress region external compressive stress was introduced into the composite samples by Vickers indentation. With this stress field both spectra: luminescence and Raman were collected at the same place on the sample at a distance of 0-300 μm from the indent. The intensity of this stress was expected to diminish with distance from the indent. As can be seen from Fig. 8, the R_2 luminescence shift strongly decreases with distance from the indent to maintain the value typical for an unidented area of the composite at 200 μm. The R_2 shift converted to stress present in the alumina due to indent is shown in Fig. 9. The compressive stress close to the indent (20 μm) reaches 723.7 MPa and then decreases with distance to achieve at 200 μm a value similar to the "natural" residual compressive stress in alumina of the same composite sample equal to 166 MPa.

Changes made by the indent in t-ZrO_2 are more complex. As a result of force equilibrium when alumina is in compression ZrO_2 should be in tension in an unidented composite sample. A high compressive stress

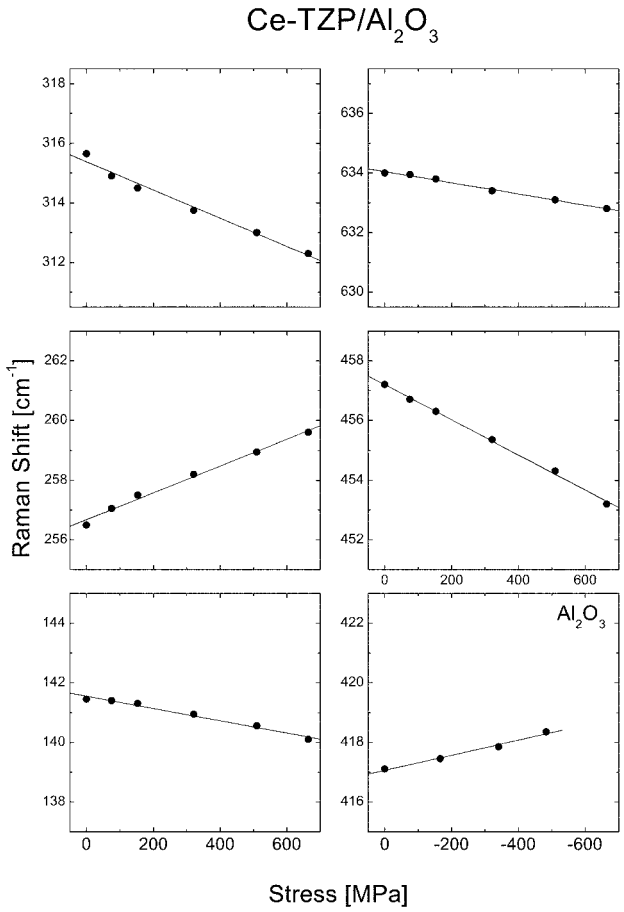

Fig. 5. Raman lines position of t-ZrO_2 as a function of its internal stress in Ce-ZrO_2/Al_2O_3 composites. In the right bottom part of the picture the same is shown for 417 cm^{-1} line of Al_2O_3.

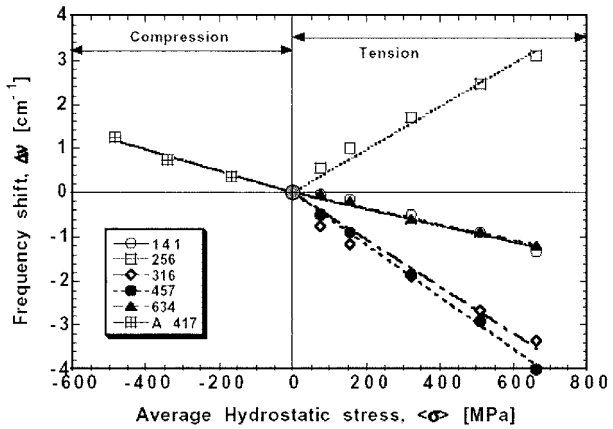

Fig. 6. Frequency shift of the Raman band versus average hydrostatic stress. The data appearing in the tensile region of the graph belong to the Raman bands of t-ZrO_2. The data appearing in the compressive region belong to the alumina Raman band at 417 cm^{-1}.

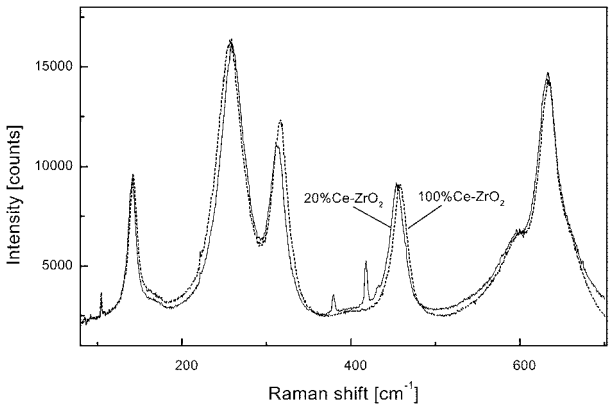

Fig. 7. Raman spectra of Ce-ZrO_2 ceramics and Ce-ZrO_2/Al_2O_3 composite containing 80 vol.% of alumina. In the spectrum of composite alumina lines are observed at 379 and 417cm^{-1}.

introduced by the indent increases the compressive stress in the alumina as shown above but changes the initial stress in the ZrO_2. Close to the indent (20 μm) a compressive stress is also observed in zirconia. This converts to a tensile one, typical for the equilibrium state, when the distance from the indent increases (Figs 10 and 11). Again, at a 200 μm distance the tensile stress in zirconia is equal to the stress observed in an unindented area of the sample. The unbalanced stress state in the neighbourhood of the indent shows that the composite material has been plastically deformed under the high load introduced with the indent. Very short microcracks at the corners of the indent and the Vickers hardness impression of the indent shown at Fig. 1 confirm the above thesis. For both components of the composite the measured stress is a sum of the compressive stress introduced by the indentation and the "natural" residual stress (compressive or tensile) generated by the difference in thermal expansion properties. This way, the compressive stress from the indentation adds to the compressive residual stress in the alumina resulting in a higher final value of the compressive stress. In the case of zirconia, the same compressive stress from the indent adds to the tensile residual stress. Close to the indent the measured compressive stress in

Table 2. Piezospectroscopic coefficients for all Raman bands of t-ZrO_2

Piezospectroscopic coefficients, cm^{-1}/GPa	Raman band, cm^{-1}					
	140	260	316	457	632	417 (Al_2O_3)
From balance formula	-2.1	+4.5	-4.7	-5.9	-1.9	-2.5
From indentation	-2.4	+3.7	-4.0	-6.5	-2.7	-1.8
Previous works					-1.83 [12] -2.4 [13]	-2.2 [11] -2.5 [10]

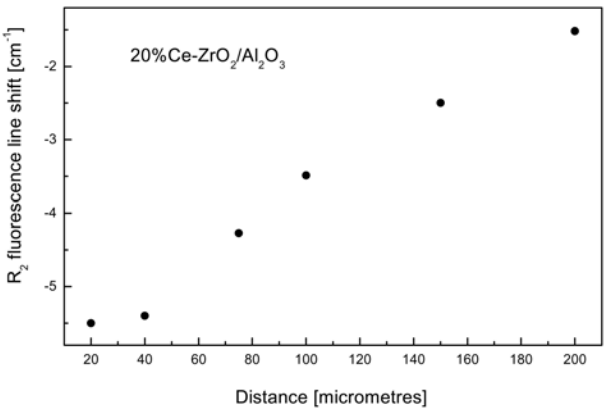

Fig. 8. R_2 luminescence shift as a function of distance from the indent made in Ce-ZrO_2/Al_2O_3 composite sample containing 80 vol.% of alumina.

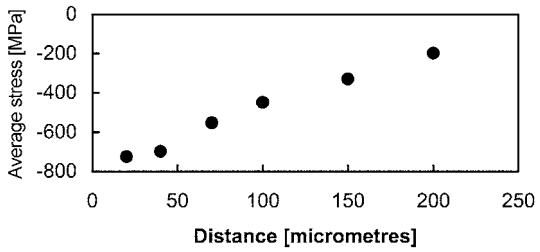

Fig. 9. Changes of compressive stress in alumina with distance from the indent for Ce-ZrO_2/Al_2O_3 composite sample containing 80 vol.% of Al_2O_3.

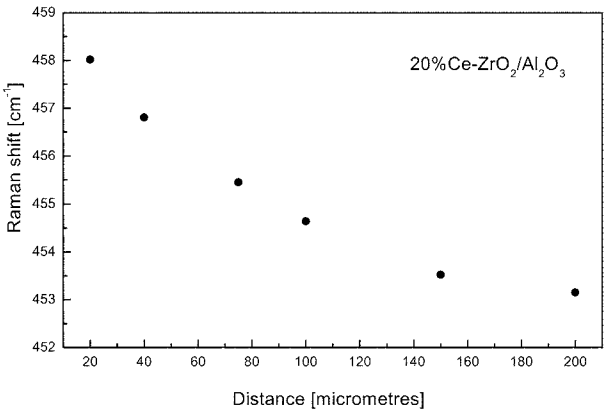

Fig. 10. Raman shift of 457 cm^{-1} band as a function of distance from the indent made in Ce-ZrO_2/Al_2O_3 composite sample containing 80 vol.% of alumina.

the t-ZrO_2 is the final result of stresses summing and changed to a tensile one when the externally introduced compressive stress decreases with increasing distance from the indent. A high external stress means that some portion of the t-ZrO_2 grains in the close neighbourhood of the indent transform to the monoclinic phase, which results in the presence of 178 and 190 cm^{-1} bands of m-ZrO_2 in the Raman spectrum (see Fig. 12). However at a distance higher than 50 μm only the tetragonal peaks of zirconia are again observed. Luminescence and Raman spectra taken from these areas (both at the

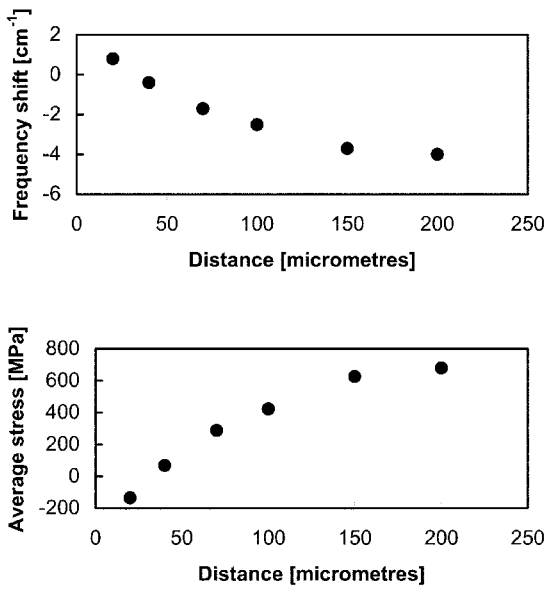

Fig. 11. Frequency shift of 457 cm^{-1} Raman band and average stress in zirconia as a function of distance from the indent made in Ce-ZrO_2/Al_2O_3 composite sample containing 80 vol.% of alumina.

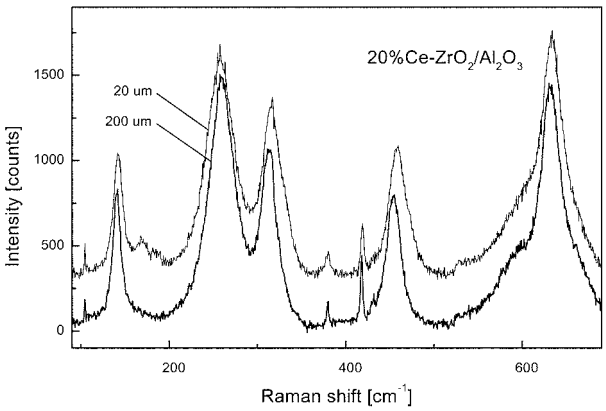

Fig. 12. Raman spectra of Ce-ZrO_2/Al_2O_3 composite sample containing 80 vol.% of alumina taken from 20 and 200 mm. distance from the indent.

same point) for all composite samples showed a linear correlation between the t-ZrO_2 Raman line shift and those of the Al_2O_3 R_2-line luminescence (see Fig. 13). The slope of the best fitting lines yields the ratio:

$$a_i = \frac{\Delta\nu_{ZrO_2}}{\Delta\nu_{Al_2O_3}} \tag{3}$$

for all corresponding Raman bands.

Eq. 2 converted to eq. 4 by introduction a_i values obtained from Fig. 13 was used for calculation new PS coefficients for all Raman bands of t-ZrO_2 and the 417 cm^{-1} band of alumina. PS coefficients determined by this method are reported in Table 2.

$$\Pi_{ZrO_2} = \frac{f_{ZrO_2}\Delta\nu_{ZrO_2}\Pi_{Al_2O_3}}{f_{Al_2O_3}\Delta\nu_{Al_2O_3}} \tag{4}$$

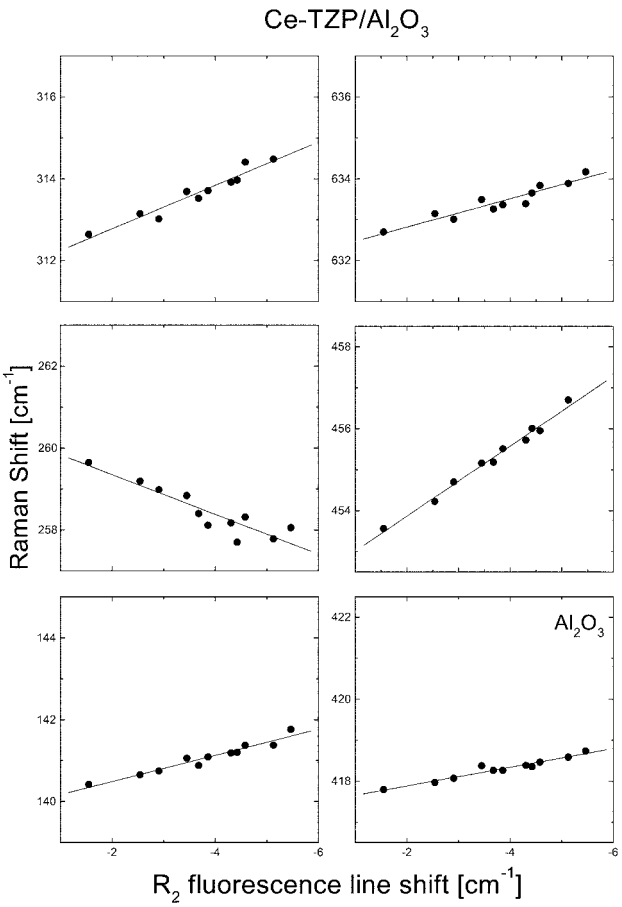

Fig. 13. The t-ZrO_2 Raman line shift versus the Al_2O_3 luminescence R_2-line shift observed in Ce-ZrO_2/Al_2O_3 composites for 20, 60 and 90 vol% of zirconia content.

The last PS data show a good agreement with those obtained by the first method and those previously published by other researchers on a more limited set of compositions. It is also evident that the bands more stress-sensitive, and hence more indicative for PS analysis, are the ones at 316 and 457 cm^{-1}. As was mentioned earlier the method of PS coefficient determination presented here rely on a knowledge of the stress in one component of the composite to retrieve the stress (and subsequently the PS coefficient) in the second one. The advantage for both of them is that the spectra have been collected from very small samples and simply sintered. Only the second one needs some machining and polishing for preparing Vickers indents.

Conclusions

The residual stresses in Ce-ZrO_2/Al_2O_3 composites containing 10-90 vol.% of alumina were measured using piezospectroscopic effects. The stress in Al_2O_3 was determined through the shift of the R_2 luminescence of Cr^{+3} and commonly known piezospectroscopic coefficient. The stress in t-ZrO_2 was calculated by two methods. In the first case the stress (and subsequent PS coefficients) was found from the equation of force equilibrium. In the second method an external stress field introduced by Vickers indent was used for new PS coefficients determination due to the linear dependence observed between the t-ZrO_2 Raman line shift and those of the Al_2O_3 R_2-line luminescence for all the Raman lines of zirconia. As a result two new indirect methods for determining the piezospectroscopic coefficient of t-ZrO_2 were suggested.

References

1. A.G. Evans, Acta Metall. 26 (1978) 1845-1853.
2. C.C. Wu, S.W. Freiman, R.W. Rice, and J.J. Mecholsky, J. Mater. Science 13 (1978) 2659-2670.
3. H. Tomaszewski, J. Strzeszewski, and W. Gebicki, J. Europ. Cer. Soc. 19 (1999) 255-262.
4. S.J. Bennison, and B.R. Lawn, Acta Metall. 37 (1989) 2659-2671.
5. H. Tomaszewski, M. Boniecki, and H. Weglarz, J. Europ. Cer. Soc. 20 (2000) 2569-2574.
6. G. Pezzotti, V. Sergo, O. Sbaizero, N. Muraki, S. Meriani, and T. Nishida, J. Europ. Cer. Soc. 19 (1999) 247-253.
7. V. Sergo, Measurements of Residual Stresses, Fourth Euro Ceramics 3, 47-54.
8. Q. Ma, and D.R. Clarke, J. Amer. Cer. Soc. 76[6] (1993) 1433-1440.
9. J. He, and D.R. Clarke, J. Amer. Cer. Soc. 78[5] (1995) 1347-1354.
10. J.A. Pardo, R.I. Merino, V.M. Oreta, J.I. Pena, C. Gonzales, J.Y. Pastor, and J. Llorca, J. Amer. Cer. Soc. 83[11] (2000) 2745-2752.
11. M.R. Gallas, Y.C. Chu, and G.J. Piermarini, J. Mater. Res. 10[11] (1995) 2817-2822.
12. J.D. Belnap, J.F. Tsai, and D.K. Shetty, J. Mater. Res. 9 (1994) 3183-3193.
13. V. Sergo, D.R. Clarke, and W. Pompe, J. Amer. Cer. Soc. 78 (1995) 633-640.
14. V. Sergo, G. Pezzotti, O. Sbaizero, and T. Nishida, Acta Mater. 46 (1998) 1701-1710.